INTERFACE CHARACTERIZATION OF PLASMA SPRAYED HYDROXYAPATITE COAT ON Ti-6Al-4V

M. Ghorbani, A. Afshar, N. Ehsani and M. R. Saeri

Department of Materials Science and Engineering, Sharif University of Technology
Azadi Avenue, P. O. Box 11365- 9466, Tehran, Iran
ghorbani@sharif.edu.ac.ir - afshar@sharif.edu.ac.ir - msaeri@cc.iut.ac.ir

C. C. Sorrell

School of Materials Science and Engineering, University of New South Wales
Sydney, NSW 2052, Australia, C.Sorrell@unsw.edu.au

(Received: January 30, 2001 – Accepted in Revised Form: April 9, 2002)

Abstract Hydroxyapatite (HA), a material proven to be biocompatible within the human body, has been produced to a high level of purity. This material has been applied as a coating on Ti-6Al-4V alloy by using the air plasma spraying technique. The coat was characterizted with SEM, XRD, FTIR and Raman spectroscopy methods to consist of a mixture of calcium phosphates including HA mainly and traces of tricalcium phosphate, tetra calcium phosphate and calcium oxide phases. This HA phase was dehydrated and partially decomposed to oxyapatite and amorphous HA. EPMA method was used cross-sectionally on the interface in order to determine the depth profiles and elemental maps of Calcium, Phosphorous, Oxygen, Titanium, Vanadium and Aluminum elements. The results clearly showed the evidence of interdiffusion at the interface. Ultimately, the diffusion depth of each element was studied and compared with each other.

Key Words Hydroxyapatite, Coat, Plasma Spraying, Interface

چکیده هیدروکسی آپاتیت که ماده‌ای با قابلیت سازگاری با محیط داخل بدن است، با خلوص بالا، سنتز گردیده و با استفاده از روش پلاسما اسپری روی زیرلایه‌ای از جنس Ti-6Al-4V پوشش داده شده است. از روشهای SEM، XRD ، FTIR و اسپکتروسکوپی Raman برای تعیین مشخصات پوشش حاصله استفاده گردید. نتایج نشان داد که پوشش، مشتمل بر هیدروکسی آپاتیت و اثراتی از فازهای تری کلسیم فسفات، تتراکلسیم فسفات و اکسید کلسیم است. فاز هیدروکسی‌آپاتیت پوشش بصورت جزئی دهیدراته شده و فاز هیدروکسی آپاتیت بهمراه فاز هیدروکسی آپاتیت آمورف تشکیل می گردد. از آنجا که هدف اصلی تحقیق حاضر مطالعه چگونگی نفوذ عناصر در سطح مقطع پوشش و زیرلایه می‌باشد؛ لذا با استفاده از روش EPMA این سطح مقطع بررسی شد. نقشه‌های عنصری و تغییرات خطی عناصر کلسیم، فسفر، اکسیژن، تیتانیم، وانادیم و آلومینیم در ناحیه فصل مشترک اندازه گیری گردید و نتایج بوضوح اثرات نفوذ این عناصر در فصل مشترک را نشان داد. همچنین عمق نفوذ این عناصر اندازه‌گیری گردیده و با یکدیگر مقایسه شدند.

1. INTRODUCTION

Bioactive calcium phosphate ceramic coating, especially hydroxyapatite coating on bioinert metallic substrates have been paid worldwide attention in both orthopedic and dental practice [1]. The brittleness of bulk hydroxyapatite ceramic makes it incapable of being used for load bearing application. On the other hand, Ti-6Al-4V is a biocompatible implant with excellent mechanical properties for load bearing situations. Several methods are available for the application of bioactive hydroxyapatite coatings. Plasma spraying technique has been most popular with ceramics

since the basic technology is well established. Animal and laboratory evaluations [1-2] and initial clinical experiences have shown satisfactory results [3]. Fast bone adaptation, firm implant-bone attachment, reduced healing time, increased tolerance of surgical inaccuracies and inhibition of ion release are some of the advantages arising from this type of coating design [2-5].

Plasma spraying will induce a series of changes to the phase composition, structure and other properties of the feeding materials, which depend on the plasma spraying conditions [5]. The temperature of the feed powder during plasma spraying is usually much higher than the melting point of hydroxyapatite [1], so it is unavoidable that quite large proportions of hydroxyapatite powder will be amorphized by plasma spraying [6].

The phase composition of the coating formed by plasma spraying depends on the thermal history of the HA powders as it passes through the flame [7]. Before any consideration of the microstructure of plasma sprayed hydroxyapatite, it is necessary to have information of the appropriate phase equilibrium. The equilibrium phase diagram for the system CaO-P_2O_5-H_2O shows that hydroxyapatite undergoes incongruent melting and decomposes at high temperature (T_1) to a mixture at tricalcium phosphate ($Ca_3(PO_4)_2$), tetracalcium phosphate Ca_4P_2O, and water (Figure 1). T_1 depends upon the partial pressure of H_2O increasing from ~1325°C to ~1550°C as the water partial pressure is increased from 6.67×10^2 to 1.33×10^4 Pa [8].

This fact has shown that the hydroxyapatite crystal structure may vary if water is partly removed to form a solid solution of hydroxyapatite and oxyapatite ($Ca_{10}(PO_4)_6O$). The range of composition at "equilibrium" is given by:

$$Ca_{10}(PO_4)_6(OH)_{2-2x}\ O_x\ \square_x$$

where $x \geq 0.75$ and $\square$ = Vacancy.

It means that 75% of the water may be lost whilst retaining the HA crystal structure. The differences in lattice parameters between hydroxyapatite and oxyapatite are reported to be small so that the structural changes arising from the loss of water are not obvious from XRD patterns. A combination of tetracalcium and tricalcium phosphate exists at high temperature and maintains a constant composition down to low temperatures. Only the structure of tricalcium phosphate will change upon cooling. The high temperature polymorph of α-tricalcium phosphate will not form on quenching but will change to β-tricalcium phosphate under slow cooling

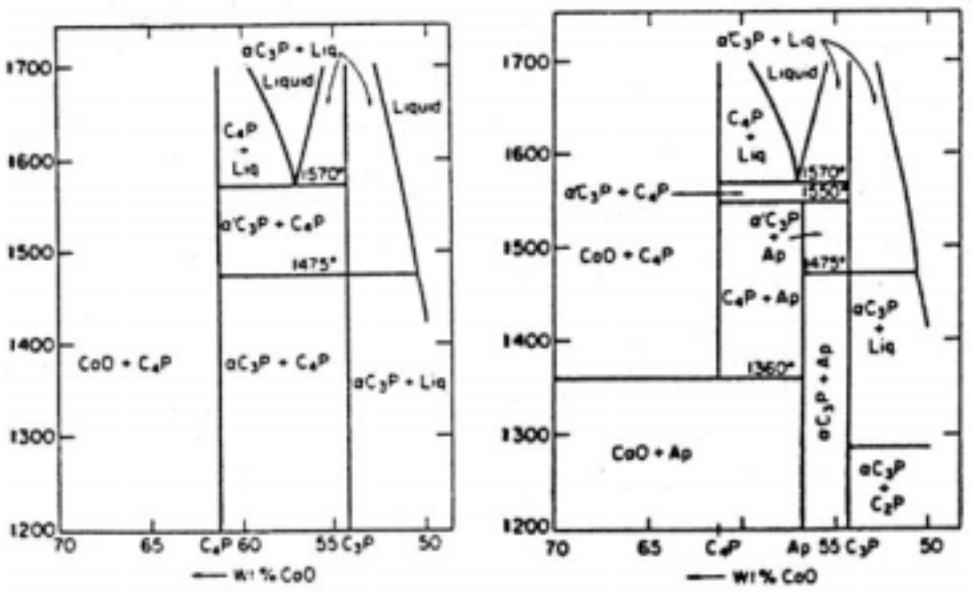

Figure 1. Phase diagram of CaO/P_2O_5 mixtures, under an atmosphere without any water (Left) and P_{H_2O}= 500 mm (Right). Vertical axis is temperature [8].

TABLE 1. Plasma Spraying Parameters Employed for Preparation of the Hydroxyapatite Coatings.

Parameters	
Argon, Flow rate (L/min)	41
Hydrogen, Flow rate (L/min)	8
Powder carrier gas, Flow rate (L/min)	3.2
Powder feed rate (g/min)	20
Power (KW)	40.2
Stand- off distance (cm)	7.5
Surface speed (cm/min)	2400
Transverse speed (cm/min)	60

conditions [7]. In the case of plasma spraying it is more probable that the α-tricalcium phosphate will be formed [9]. If the partial water pressure is sufficiently high, hydroxyapatite is introduced as a stable stoichiometric compound [7]. Decomposition of hydroxyapatite could be according to the following reactions [10, 11]:

$$2HA \rightarrow 2Ca_2(PO_4)_2 + Ca_4P_2O_9 + H_2O$$
$$2HA \rightarrow 3Ca_3(PO_4)_2 + CaO + H_2O$$

The decomposition product types are related to impurity and stoichiometry of hydroxyapatite [8,12].

The majority of the studies involving hydroxyapatite coatings have focused on the hydroxyapatite-bone interface, but the success of load-bearing implants as used in orthopedics and dentistry relies equally on the maintenance of an integral structure at the hydroxyapatite-metal substrate interface [13].

Recent studies have demonstrated that the metal/ceramic interface is an important part of the plasma sprayed hydroxyapatite-coated Ti-6Al-4V system and may; in fact, represent the "weakest link" in implant design. Ceramics may be used in highly stressed applications, such as hip and knee implants when they are applied as coatings [14]. In general, the interfacial bond strength between ceramics and metals depends on chemical reactions, which take place at the interface. The evidence of some elemental interdiffusion at the hydroxyapatite-Ti alloy interface contradicts the widely held belief of a purely mechanical bond in plasma-sprayed ceramic-metal substrate systems [13]. However it is not clear whether interfacial reactions occur do in fact [15].

In this work the microstructure and chemical and distribution was measured in a particle size analyzer (Master Sizer/G, Malven Instrument Inc.). As shown in Figure 2, the particle sizes were between 60-150 microns. Figure 3 shows the compact and semi angular surface morphology of the particles.

2.2 Atmospheric Plasma Spraying Plates of Ti-6Al-4V alloy (ASTM F-136), measuring ($3\times3\times1.58$ cm^3), were degreased and grit blasted with Al_2O_3 powder (0.7-1 mm) to roughen the surface. High purity argon at a flow rate 3.2 lit/min was used to carry the hydroxyapatite feed powder at about 20 g/min from a powder feeder to the plasma tourch of a plasma spraying system (Plasma Technik A3000S with F4-HB Tourch). By adjusting

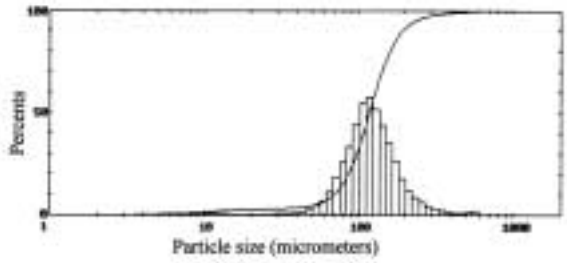

Figure 2. Size distribution of the hydroxyapatite feed powder particles.

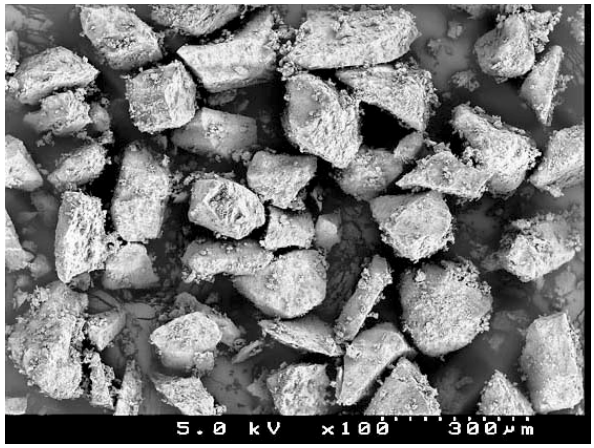

Figure 3. The SEM micrograph of hydroxyapatite feed powder particles (×100).

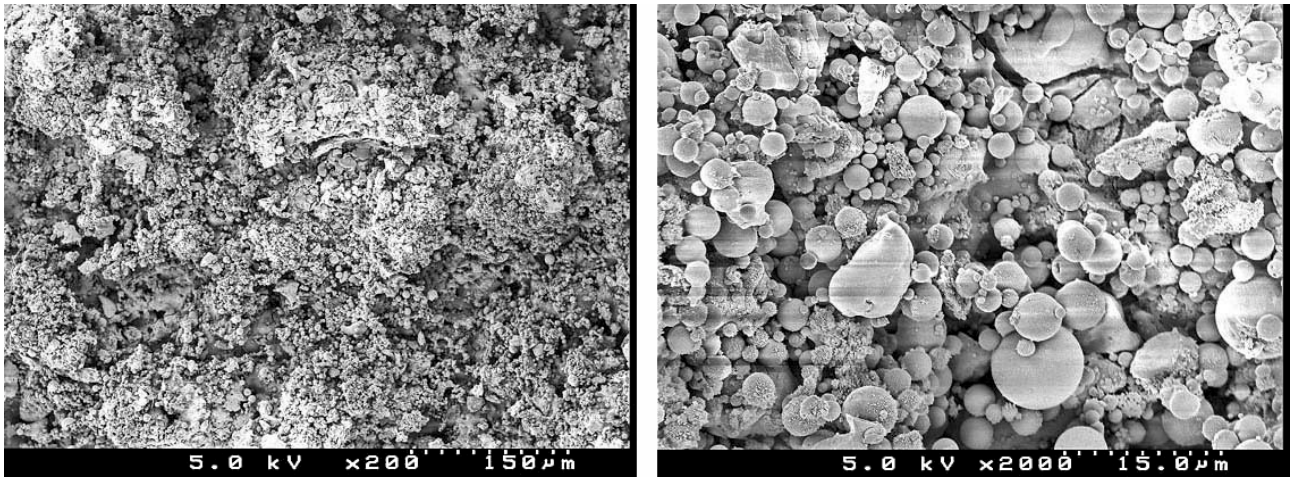

Figure 4. The surface morphology of plasma sprayed hydroxyapatite coating on Ti-6Al-4V. Micrographs obtained at various magnifications. The structure contained molten accumulated splats and a few porosity, microcrack and unmelted particle.

the spraying parameters (Table 1), the HA coating of about 100 micrometers thickness on Ti-6Al-4V were prepared.

2.3 Characterization The hydroxyapatite coat was inspected by SEM (HITACHI-S4500) at an accelerating voltage 20 KV. The melting characteristics of the coating were assessed from the surface morphology.

The phase constituents of the coat were identified by X-ray diffraction. A monochromatic copper K_α (Wave length = 1.5418 Å) was selected. The operational tube voltage and current was 30 kV and 30 mA (Siemens Diffractometer D5000, Germany). Crystalline phases present in the powders were identified by comparing their diffraction patterns and corresponding intensities with data from ASTM standards such as Hydroxyapatite; JCPDS 9-432, α-C3P; JCPDS 9-348, β-C3P; JCPDS 9-169 & 32-176 & JCPDS 2-649, C4P; JCPDS 25-1137, CaO; JCPDS 37-1497 & 43-1001 & 28-775 and $Ca_2P_2O_7$; JCPDS 2-647.

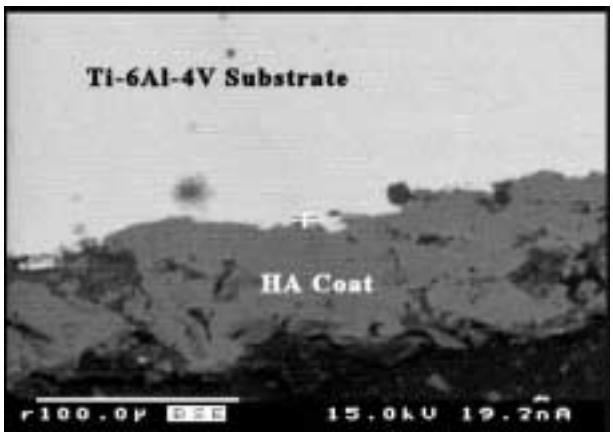

Figure 5. Cross-sectional view of plasma sprayed hydroxyapatite coating on Ti-6Al-4V.

The samples were prepared by pressing a small amount of the scraped HA coat into standard KBr powders. The chemical nature and molecular bond structure of the coat were determined from the measured FTIR (ATI MATTSON, Gensis series FTIR Spectrometer) The IR spectrum offers direct molecular information on structure and composite for identification of different phases. The FTIR method can detect the dehydrated and carbonate-doped hydroxyapatite but XRD methods do have not this ability. Furthermore the shape and split of the IR band can be related to the crystallity of the material [18]. The basic of the ability of FTIR method for analysis is that the infrared absorption depends on the molecular vibrational energy levels. Depending on the symmetry, some molecular vibrations are Raman active and infrared inactive and vice versa [19]. Hence infrared (FTIR) and Raman spectroscopy give complementary information about the crystallization state of the sample [20].

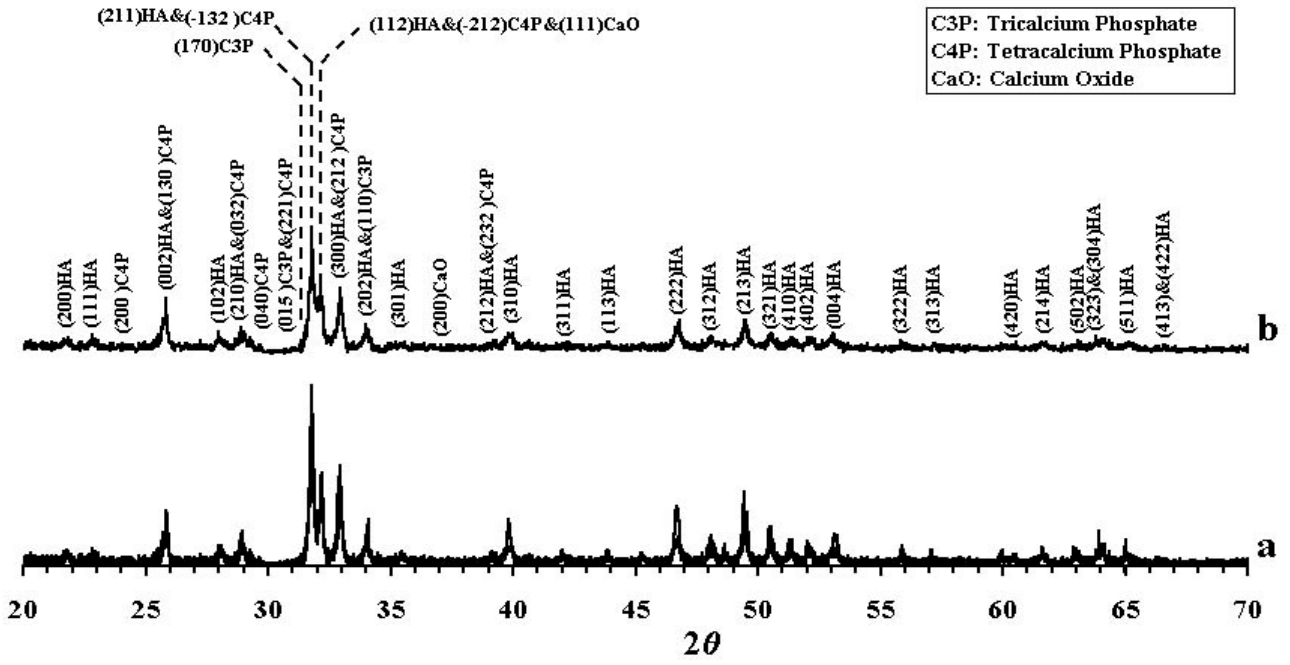

Figure 6. Typical XRD pattern of the feeding hydroxyapatite powder (a) and plasma sprayed hydroxyapatite coating (b). Notice that peaks of each intermediate phase as well as that of hydroxyapatite were labeled.

Raman spectra were performed on some as-precipitated and sintered samples of synthesized Hydroxyapatite. The Raman spectra were measured using the argon greens line at 514.5 nm, with laser power of 20 mW and exciting wavelength 514.532 nm (Renishaw Raman scope, Raman group, Renishaw PLC). This output was within the range of power levels, which do not incur any noticeable specimen damage [21]. Microstructure features were identified on a light microscope with a 50× microscope objective. A 20-sec collection time was used for acquiring the spectrum.

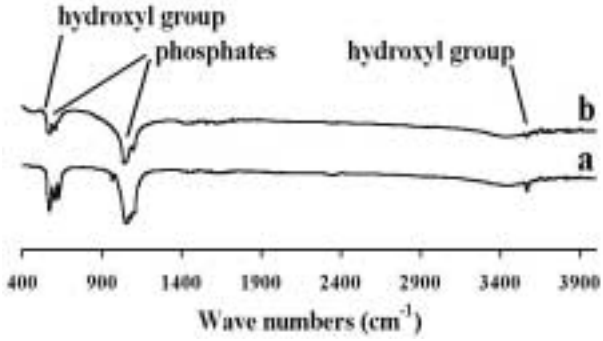

Figure 7. Typical FTIR spectra of the hydroxyapatite feed powder (a) and plasma sprayed hydroxyapatite coating (b).

Electron probe microanalysis (Universal EPMA, CAMECA SX50 analyzer) was carried out on specimens that were ground and diamond polished normal to the metal ceramic interface. The operational voltage and current were 15 kV and 20 nA respectively. Care was taken to avoid excessive coating pullout and delamination during the grinding operation. Chemical analyses were obtained in depth profile (2 nm intervals) and qualitative elemental map forms. Calcium, Phosphorous, Oxygen, Titanium, Vanadium and Aluminum were measured with high accuracy. The microstructures of the coating were also examined cross-sectionally by the back scattering electron image technique (BEI).

3. RESULTS AND DISCUSSION

The microstructures of the coated samples were examined by SEM. The surface morphology was a well molten coating with accumulated splats and porosity (Figure 4). The cross section of typical

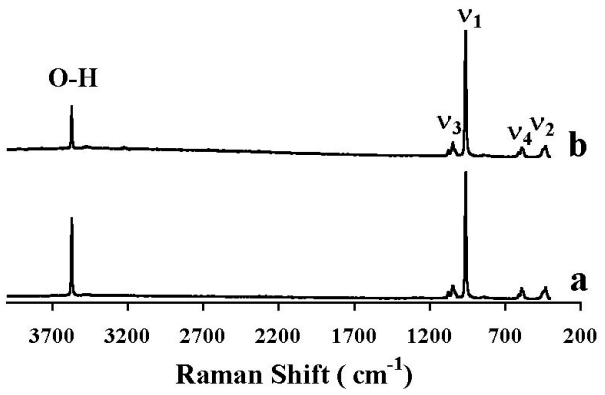

Figure 8. Typical Raman spectra of the hydroxyapatite feed powder (a) and plasma sprayed hydroxyapatite coat (b).

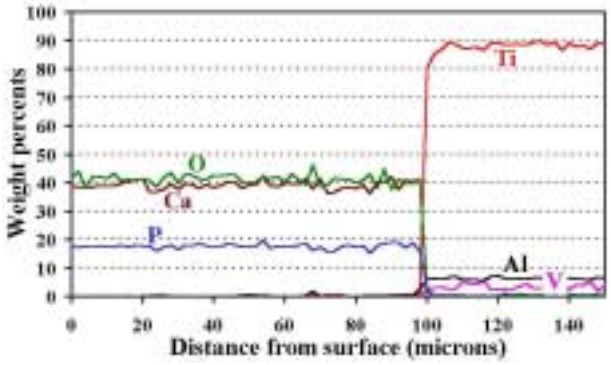

Figure 9. Typical depth profiles (EPMA line scan) of Calcium, Phosphorous, Oxygen, Titanium, Vanadium and Aluminum concentration (wt%) of Ti-6Al-4V surface, which, was coated with hydroxyapatite.

hydroxyapatite coated sample is shown in Figure 5. It can be seen that the coating is built up of layers of flattened particles with porosity and micro cracks. During the plasma spraying process, the hydroxyapatite particles are injected into an argon gas system and carried into a plasma flame, which totally melt or soften the surface of the particles. When these particles impact on the substrate at a high velocity, they become flattened and adhere to the surface by mechanical interlocking. The laminated structure produced is typical of plasma sprayed coatings [22].

Typical X-ray diffraction patterns of the hydroxyapatite feed powder obtained from the surface of the coating are shown on Figure. 6. The full width at half maximum (FWHM) and background of XRD pattern for hydroxyapatite increased after plasma spraying compared to the feed powder. This reveals that the crystallinity of hydroxyapatite in the coating has decreased [23]. The X-ray diffraction pattern of the coating matches the standard diffraction pattern for pure hydroxyapatite. Also traces of tricalcium phosphate, tetracalcium phosphate and calcium oxide, which are labeled in Figure 6, were found in the coating.

The corresponding bonding analysis of the hydroxyapatite feed powder and the plasma sprayed coat are shown in Figure 7. Most of the peaks are attributed to tree vibration modes [24]:

1. The stretching modes of $(PO_4)^{3-}$ occurring at 962 and 1046 cm $^{-1}$
2. Two or three bending modes of $(PO_4)^{3-}$ occurring at 576 and 600 cm $^{-1}$
3. The stretching mode of OH^- occurring at about 3570 cm $^{-1}$, shown as a small shoulder of the large H-O-H (3400 cm $^{-1}$) peak.

After plasma spraying of the calcined powder the intensity of OH peaks and the background of the powder in the high-energy region were decreased (Figure 7).

All the characteristic features like a very weak OH^- band at 3570 cm^{-1} and the absence of hydroxyl band at 633 cm^{-1}, two medium intensity bands at 970 and 946 cm^{-1}, bands at 604, 582 and 568 cm^{-1}, a shoulder at 556 cm^{-1}in a bending vibration mode of PO4 group, and a medium intensity band at 481 cm^{-1} are indications of oxyapatite formation [24].

The crystallinity of hydroxyapatite can be estimated from the FTIR based on the splitting resolution of the two or three peaks near 600 cm^{-1} [18]. A comparison between Figures 6a and 6b showed that the crystallinity of the hydroxyapatite feed powder was decreased and after plasma spraying (over 70 percent vs. 50 –70 percent).

Figure 8 shows the Raman spectrums of the hydroxyapatite feed powder and plasma sprayed hydroxyapatite. The spectrums of the samples were overlaid with that of pure hydroxyapatite spectrum [20, 25, 26]. The strongest intensity band at 962 cm^{-1} is assigned to ν_1; the strong bonds at 590 and 565 cm^{-1} and the shoulder at 571 cm^{-1} are assigned to a factor group components of ν_4; the medium bands at 1070 and 1040 cm^{-1} are assigned to ν_3, the weak band at 470 cm^{-1} (in contrast to the previous assignments) can be attributed to ν_2 and the medium intensity band at 3570 cm^{-1} to an OH vibrational mode [21].

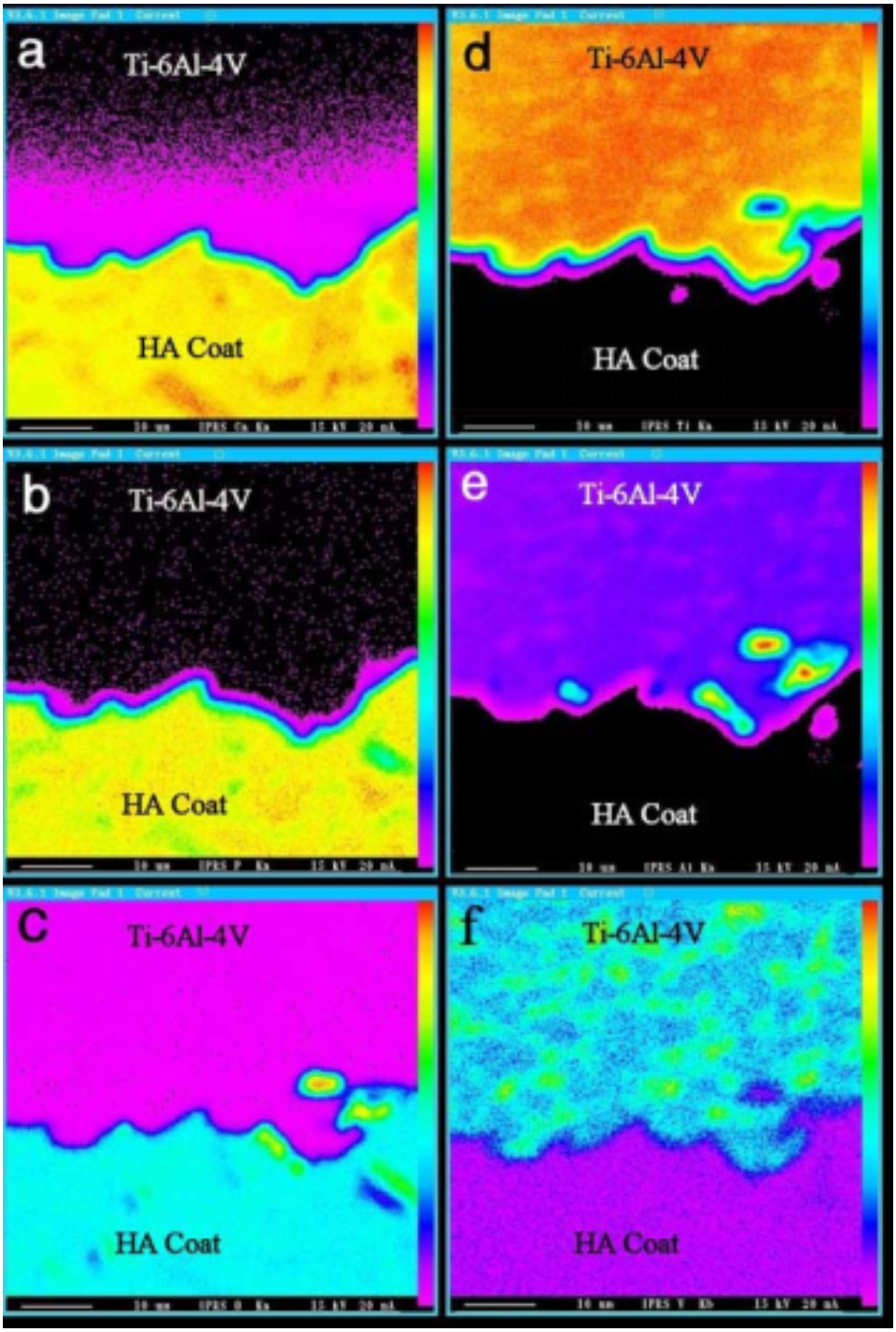

Figure 10. EPMA mapping of the plasma sprayed hydroxyapatite coating/Ti-6Al-4V interface for (f) Vanadium. (a) Calcium, (b) Phosphorous, (c) Oxygen, (d) Titanium, (e) Aluminum and Colors show concentration of particular elements. The concentration increases from black color (~0%) to red color (~100%). Notice more interdiffusion depth of (a) Calcium compared with that of (b) Phosphorous.

The Raman spectrums clearly showed that the intensity of O-H peak was decreased after plasma spraying. This finding represents that some hydroxyl groups have been removed from the

apatite [27]. Based on Weinlender and his co-workers' experiments [21], the FWHM of ν_1 peak is directly related to the degree of long-range order and/or amount of crystalline phases. The FWHM of the strongest Raman peak (ν_1) was decreased after plasma spraying coat (11.9 vs. 11.1 cm^{-1}). These findings denote the crystallinity [27,28] and/or the long rang order [21] of hydroxyapatite was decreased after plasma spraying. Comparing the Raman spectrum of the plasma sprayed coat with that of tricalcium phosphate [21,26,28], there was no indication of tricalcium phosphate peaks.

The depth profiles of Calcium, Phosphorous, Oxygen, Titanium, Vanadium and Aluminum elements are shown in Figure 9. This figure shows the variations in concentration values of elements in the coating have a larger tolerance compared to another parts. As the SEM results showed the coating is built up of layers of the flattened particles with porosity and micro cracks. It was also suggested that the different parts of the plasma sprayed particles have a different thermal history during plasma spraying. This can lead to different structures of the flatted particles [22 and ultimately, wide tolerance range variation in chemical composition in the coat region (Figure 9). Also Calcium, Oxygen and Phosphorous depth profiles show a diffusional gradient at the hydroxyapatite/Ti alloy interface.

The mapping of various elements at this interface is presented in Figure 10. Relative elemental concentration gradients can be estimated from different colors for particular elements. Generally, there was discernable elemental inter-diffusion indicative of chemical bonding for this system and it was interesting to see good bonding between the coating and metallic substrate.

The existence of a diffusional interface following sintering of hydroxyapatite coated Ti alloy samples has been proposed by Duchyne et al. [30 involving sintering of hydroxyapatite powder that were electrophoretically deposited onto the surface of commercially pure Titanium. However, as the coating method has been different and the characterization has been made on sintered samples it is difficult to compare their results with the present one.

Of course, the dynamics of the plasma spraying process, in which splat solidification was reported to occur at the order of 10^4 to 10^6 °C/s for ceramics [13] then limiting the extent of diffusion. However with enhanced localized heating at thermally isolated asperities or protrusions. The low thermal conductivity of ceramics, and the fairly rapid application of successive molten ceramic layers during plasma spraying mean that the existence of localized diffusion on this scale is not unreasonable.

As Figures 10d, 10e and 10f show, little Titanium, Vanadium and Aluminum diffusion into the coating were evident as indicated by the well-defined edges of the elemental maps for them. For this analysis, Titanium, Vanadium and Aluminum were superimposed over each others' net elemental maps and the results showed that the depth of diffusion increased in the following order: Vanadium, Aluminum and Titanium. The possibility of Titanium diffusing into the amorphous calcium phosphate layer has been reported previously [15 and 29

Superimposing the Calcium map over the corresponding Vanadium map revealed significant Calcium interdiffusion into the metal substrate to a depth of 2-3 microns (Figure 10a). Diffusion depths of Oxygen and Phosphorous were measured by following the same procedure. The results show more interdiffusion of Oxygen (1-2 microns) compared to Phosphorous (<1 micron).

Only a few studies have been done on measuring the interdiffusion depths at the hydroxyapatite/Ti alloy interfaces. Huaxia et al. studied the coating adjacent to the interface by TEM. They found an amorphous phase with a Ca/P = 0.7 [9], which can be taken as evidence of more calcium diffusion from hydroxyapatite coat to the metallic substrate. Their findings are in agreement with the findings of the present study.

Filiggi et al. studied the hydroxyapatite/Ti-6Al-4V interface using Electron Spectroscopic imaging (ESI) technique and could only detect [13, 14] a (~1-2 micron) interdiffusion depth for Phosphorous by this method. They implied that this depth might have been exaggerated with the loss of coating at the interface during specimen preparation, exposing the ''diffusion" zone to an incident beam not normal to the cross section plane [14]. Thus, they could not find any significant diffusion of Calcium into the Titanium alloy, they have explained this on the ground, that Phosphorous has a smaller ionic radius

compared to Calcium, (0.35 Å vs. 0.99 Å for Ca), then would been expected to diffuse more rapidly into the Ti-6Al-4V alloy or along the oxide grain boundaries [13,14]. Similar to our results, they reported the extent of the Titanium-Phosphorous overlap zone (~1-2 microns), but suggested Phosphorous diffuse into the alloy and/or surface oxide film along grain boundaries [13]. Huxia et al. suggested that the Phosphorous compound was transformed into the crystalline calcium phosphate with a lower phosphorous content, as phosphorous ions diffuse into the titanium and amorphous phase. Then some chemical bonding could be generated at the interface although the majority of the bonding is likely to remain the mechanical interlocking producing by the plasma-spraying process [9]. However, a number of researchers suggested [6,9,31 that high-resolution analysis demonstrated a diffusion zone and this supports the notion of some chemical interaction at the hydroxyapatite/Ti alloy interface. They suggested that under oxidizing conditions the hydroxyapatite would be transformed to tricalcium phosphate as the titanium oxide produced removes calcium ions through the formation of calcium titanium oxide ($CaTi_2O_5$) as shown in the following reaction [9]:

$$(n+1)\ Ca_{10}(PO_4)(OH)_2 + 2nTiO_2 \rightarrow (n-1)\ Ca_{10}\text{-}(PO_4)(OH)_2 + 3nCa_3(PO_4)_2 + nCaTi_2O_5 + 2H_2O$$

Furthermore, Sorrell et al. reported that Titanium decrease the deposition temperature of hydroxyapatite [32]. Thus it is expected to have some tricalcium phosphate and $CaTi_2O_5$ phases at the interface.

In the present study, the Ca/P ratios of the coat at the interface were investigated and it was found that this ratio was increased to ~2 in some places at the interface. This could relate to presence of tricalcium phosphate. Filliaggi et al. implied that results from qualitative x-ray microanalysis of the failed surfaces and from chemical mapping (EDX, ESI) in their similar study reported that this interface consisted predominantly of tetracalcium phosphate ($Ca_4P_2O_7$), which possesses a higher Ca/P ratio than HA or/and the observed Phosphorous diffusion into the Ti-6Al-4V substrate [14].

4. SUMMARY

Plasma spraying technique has been successfully applied to coat of hydroxyapatite on Ti-6Al-4V substrate. An attempt has been made to characterize the metal-ceramic interface, which constitutes an important part of the plasma sprayed hydroxyapatite coating on a Ti-6Al-4V substrate. Evidence of an interdiffusion region at this interface was revealed, using an EPMA method.

For this analysis, Calcium, Phosphorous and Oxygen were superimposed over the original Titanium elemental map and the results showed that the depth of diffusion increased in the following order: Phosphorous, Oxygen and Calcium. Little Titanium, Vanadium and Aluminum. Diffusion into the coating was evident as indicated by the well-defined edges of the elemental maps for Titanium. The depth of diffusion of the substrate elements to the coat increased in the following order: Aluminum, Vanadium and Titanium.

Further investigation is needed to confirm the trends reported herein. Still, this preliminary study does demonstrate the potential benefits of using EPMA with respect to interface chemical properties while highlighting possible shortcomings.

5. REFERENCES

1. Hench, L. L. and Wilson, J., "An Introduction to Bioceramics", World Scientific Publication Co. Pte. Ltd, Singapore, (1993).
2. Duchyne, P. and Healy, K. E., "The Effect of Plasma-Sprayed Calcium Phosphate Ceramic Coatings on the Metal Ion Release from Porous Titanium and Cobalt-Chrome Alloys", ***J. Biomed. Mater. Res.***, Vol. 22, (1988), 1137-1163.
3. Kay, J. F., "Bioactive Surface Coatings for Hard Tissue Biomaterials", in CRC Handbook of Bioactive Ceramics, Vol. 2, (Eds. T. Yamamura, L. L. Hench and J. Wilson), CRC Press, Boca Raton, Florida, (1990), 111-121.
4. Kay, J. F., "Designing to Cunteract the Effects of Initial Device Instability: Materials and Engineering", ***J. Biomed. Mater. Res.***, Vol. 22, (1988), 1127-1135.
5. Wang, J., Liu, X., Zhang, X., Ma, Z., Ji, X. and Zyman, Z., "Further Studies on the Plasma-Sprayed Amorphous Phase in HA Coatings and Its Deamorphization", ***Biomaterials***, Vol. 14, (1993), 578-582.
6. Weng, J., Liu, X., Zhang, X. and De-Groot, K., "Integrity and Thermal Decomposition of Apatite in Coatings Influenced by Underlying Titanium During Plasma Spraying and Post-Heat-Treatment", ***J. Biomed. Mater. Res.***, Vol.30, (1996), 5-11.
7. Gross, K. A. and Berndt, C. C., "Thermal Processing of HA for Coating Production", ***J. Biomed. Mater. Res.***, Vol. 39, (1998), 580-587.
8. Lacout, J. L., "Calcium Phosphate as Bioceramics" in Muster D. (ed.), Biomaterials: Hard Tissue Repair and Replacement, Elsevier Science Publishers B. V., (1992),

83-95.
9. Huaxia, J. I., Ponton, C. B. and Marquis, P. M., "Micro Structural Characterization of HA Coating on Titanium", ***J. Mater. Sci. - Mater. Med.***, Vol. 3, (1992), 283-287.
10. Bouyer, E., Gitzhofer, F. and Boulos, M. I., "The Suspension Plasma Spraying of Bioceramics by Induction Plasma", ***JOM***, (Feb.1997), 58-62.
11. Chen, J., Tong, W., Cao, Y., Feng, J. and Zhang, X., "Effect of Atmosphere on Phase Transformation in Plasma Sprayed HA Coatings During Heat Treatment", ***J. Biomed. Mater. Res.***, Vol.34, (1997), 15-20.
12. McPherson, R. et al., "Structural Characterization of the Plasma Sprayed HA Coatings", ***J. Mater. Sci. - Mater. Med.***, Vol. 6, (1995), 327-324.
13. Filiggi, M. J., Coombs, N. A. and Pilliar, R. M., "Characterization of the Interface in the Plasma Sprayed HA Coating/Ti-6Al-4V Implant System", ***J. Biomed. Mater. Res.***, Vol. 25, (1991), 1211-1229.
14. Filiggi, M. J., Pilliar, R. M. and Coombs, N. A., "Post-Plasma-Spraying Treatment of the HA Coating/Ti-6Al-4V Implant System", ***J. Biomed. Mater. Res.***, Vol.27, 1993, 191-181.
15. Park, E., Condrate, S. R. A., Hoelzer, D. T. and Fischman, G. S., "Interface Characterization of Plasma Sprayed Coated Calcium Phosphate on Ti-6Al-4V", ***J. Mater. Sci. - Mater. Med.***, Vol. 9, (1998), 643-649.
16. Berndt, C. C., Haddad, G. N., Farmer, J. D. and Gross, K. A., "Review article; Thermal spraying for bioceramic application", ***Mater. Forum***, Vol.14, (1990), 161-173.
17. Weng, B. C., Chang, E., Lee, T. M. and Yang, Y., "Changes in Phases and Crystallinity of Plasma-Sprayed HA Coating Under Heat Treatment: A Quantitative Study", ***J. Biomed. Mater. Res.***, Vol. 29, (1995), 1483-1492.
18. Flohr, K. W., "Techniques for Characterization and Quality Control of HA Raw Materials and Coating" in Horowtiz E., et al. (Ed.), Characterization and Performance of Calcium Phosphate Coatings for Implants, STP 1196, ASTM, Philadelphia, (1994), 16-24.
19. Clothup, N. B., "Introduction to Infrared and Raman Spectroscopy", Academic Press Inc., (1964), 27-29.
20. Penel, G., Leroy, G., Rey, C., Sombert, B., Huvenne, J. P. and Bres, E., "Infrared and Raman Micro Spectrometry Study of Flour-Flour-Hydroxy and Hydroxy-Apatite Powders", ***J. Mater. Sci. - Mater. Med.***, Vol. 8, (1997), 271-276.
21. Weinlaender, M., Beumer, J., Kenney, E. B., Moy, P. K. and Adar, F., "Raman Microprobe Investigation of Calcium Phosphate Phases of Three Commercially Available Plasma Flame-Sprayed HA Coated Dental Implants", ***J. Mater. Sci. - Mater. Med.***, Vol. 3, (1992), 397-401.
22. Taylor, M. P., Chandler, P. and Marquis, P. M., "The Influence of Powder Morphology on the Microstructure of Plasma Sprayed HA Coatings", ***Bioceramics***, Vol.6, Edited by P. Duchyne and D. Christiansen (Proc. of the 6th Internat. Sym. on Ceram. in Med.), Butterworth-Heinemann Ltd., (1993), 185-190.
23. Tong, W., Yang, Z., Zhang, X., Yang, A., Feng, J., Cao, Y. and, Chen, J., "Studies on Diffusion Maximum in X-Ray Diffraction Patterns of Plasma Sprayed HA Coatings", ***J. Biomed. Mater. Res.***, Vol. 40, 1998, 407-413.
24. Radin, S. R. and Ducheyne, L., "Plasma Spraying Induced Changes of Calcium Phosphates Ceramic Characteristics and the Effect on In-Vitro Stability", ***J. Mater. Sci. - Mater. Med.***, Vol. 3, (1992), 33-42.
25. Sergo, V., Sbaizero, O. and Clark, D., "Mechanical and Chemical Consequences of the Residual Stresses in Plasma Sprayed HA Coatings", ***Biomaterials***, Vol. 18, (1997), 477-482.
26. De Aza, P. N., Santos, C., Pazo, A., De Aza, S., Cusco, R. and Artus, L., "Vibrational Properties of Calcium Phosphate Compound; 1. Raman Spectrum of β-Tricalcium Phosphate", ***Chem. Mater.***, Vol. 9, (1997), 912-915.
27. Cao, Y., Weng, J., Chen, J., Feng, J., Yang, Z. and Zhang, X., "Water Vapor-Treated HA Coatings After Plasma Spraying and Their Characteristics", ***Biomaterials***, Vol. 17, (1996), 419-424.
28. De Aza, P. N., Santos, C., Pazo, A., De Aza, S., Cusco, R. and Artus, L., "Vibrational Properties of Calcium Phosphate Compound; 1. Comparison Between HA and β-Tricalcium Phosphate", ***Chem. Mater.***, Vol. 9, (1997), 915-922.
29. Wie, M., PhD thesis, University of New South Wales (1987).
30. Duchyne, P., Van Raemdonk, W., Heughbaert, J. C. and Heughbaert, M., "Structural Analysis of HA Coatings on Titanium", ***Biomaterials***, Vol. 7, (1986), 97-103.
31. Kaciulis, S., Mttogno, G., Napoli, A., Bemporad, E., Ferrari, F., Montenero, A. and Gnappi, G., " Surface Analysis of Biocompatible Coatings on Titanium", ***J. Electron. Spectrosc. Relat. Phenom.***, Vol. 95, (1998), 61-69.
32. Ruys, A. J., Ehsani, G. N., Milthorpe, B. K. and Sorrell, C. C., "Effects of Non-Oxide Additions on the Decomposition and Densification of HA" ***J. Australian Ceram. Soc.***, Vol. 29, (1993), 65-69.